
Making Deep Q-learning Methods Robust to Time Discretization

Corentin Tallec¹ Léonard Blier^{1,2} Yann Ollivier²

Abstract

Despite remarkable successes, *Deep Reinforcement Learning* (DRL) is not robust to hyperparameterization, implementation details, or small environment changes (Henderson et al. 2017, Zhang et al. 2018). Overcoming such sensitivity is key to making DRL applicable to real world problems. In this paper, we identify sensitivity to *time discretization* in near continuous-time environments as a critical factor; this covers, e.g., changing the number of frames per second, or the action frequency of the controller. Empirically, we find that *Q*-learning-based approaches such as *Deep Q-learning* (Mnih et al., 2015) and *Deep Deterministic Policy Gradient* (Lillicrap et al., 2015) collapse with small time steps. Formally, we prove that *Q*-learning does not exist in continuous time. We detail a principled way to build an off-policy RL algorithm that yields similar performances over a wide range of time discretizations, and confirm this robustness empirically.

1. Introduction

In recent years, *Deep Reinforcement Learning* (DRL) approaches have provided impressive results in a variety of domains, achieving superhuman performance with no expert knowledge in perfect information zero-sum games (Silver et al., 2017), reaching top player level in video games (OpenAI 2018b, Mnih et al. 2015), or learning dexterous manipulation from scratch without demonstrations (OpenAI, 2018a). In spite of those successes, DRL approaches are sensitive to a number of factors, including hyperparameterization, implementation details or small changes in the environment parameters (Henderson et al. 2017, Zhang et al. 2018). This sensitivity, along with sample inefficiency, largely prevents DRL from being applied in real world settings. Notably, high sensitivity to environment parameters

prevents transfer from imperfect simulators to real world scenarios.

In this paper we focus on the sensitivity to time discretization of DRL approaches, such as what happens when an agent receives 50 observations and is expected to take 50 actions per second instead of 10. In principle, decreasing time discretization, or equivalently shortening reaction time, should only improve agent performance. Robustness to time discretization is especially relevant in *near-continuous* environments, which includes most continuous control environments, robotics, and many video games.

Standard approaches based on estimation of state-action value functions, such as *Deep Q-learning* (DQN, Mnih et al. 2015) and *Deep deterministic policy gradient* (DDPG, Lillicrap et al. 2015) are not at all robust to changes in time discretization. This is shown experimentally in Sec. 5. Intuitively, as the discretization timestep decreases, the effect of individual actions on the total return decreases too: $Q^*(s, a)$ is the value of playing action a then playing optimally, and if a is only maintained for a very short time its advantage over other actions will be accordingly small. (This occurs even with a suitably adjusted decay factor γ .) If the discretization timestep becomes infinitesimal, the effect of every individual action vanishes: there is no continuous-time *Q*-function (Thm. 2), hence the poor performance of *Q*-learning with small time steps. These statements can be fully formalized in the framework of continuous-time reinforcement learning (Sec. 3) (Doya, 2000; Baird, 1994).

We focus on continuous time because this leads to a clear theoretical framework, but our observations make sense in any setting in which the value results from taking a large number of small individual actions. Our results suggest standard *Q*-learning will fail in such settings without a delicate balance of hyperparameter scalings and reparameterizations.

We are looking for an algorithm that would be as invariant as possible to changing the discretization timestep. Such an algorithm should remain viable when this timestep is small, and in particular admit a continuous-time limit when the discretization timestep goes to 0. This leads to precise design choices in term of agent architecture, exploration policy, and learning rates scalings. The resulting algorithm is shown to provide better invariance to time discretization than vanilla DQN or DDPG, on many environments (Sec. 5).

¹Tackling the Underspecified, Université Paris Sud
²Facebook Artificial Intelligence Research. Correspondence to: Corentin Tallec <corentin.tallec@u-psud.fr>, Léonard Blier <leonardb@fb.com>.

On a new environment, as soon as the order of magnitude of the time discretization is known, our analysis readily provides relevant scalings for a number of hyperparameters.

Our contribution is threefold:

- Building on (Baird, 1994), we formally show that the Q -function collapses to the V -function in near-continuous time, and thus that standard Q -learning is ill-behaved in this setting.
- Our analysis of properties in the continuous-time limit leads to a robust off-policy algorithm. In particular, it provides insights on architecture design, and constrains exploration schemes and learning rates scalings.
- We empirically show that standard Q -learning methods are not robust to changes in time discretization, exhibiting degraded performance, while our algorithm demonstrates substantial robustness.

2. Related Work

Our approach builds on (Baird, 1994), who identified the collapse of Q -learning for small time steps and, as a solution, suggested the Advantage Updating algorithm, with proper scalings for the V and advantage parts depending on timescale δt ; testing was only done on a quadratic-linear problem.

We expand on (Baird, 1994) in several directions. First, we modify the algorithm by using a different normalization step for A , which forgoes the need to learn the normalization itself, thanks to the parameterization (27). Second, we test Advantage Updating for the first time on a variety on RL environments using deep networks, establishing Deep Advantage Updating as a viable algorithm in this setting. Third, we provide formal proofs in a general setting for the collapse of Q -learning when the timescale δt tends to 0, and for the non-collapse of Advantage Updating with the proper scalings. Fourth, we also discuss how to obtain δt -invariant exploration. Fifth, we provide stringent experimental tests of the actual robustness to changing δt .

Our study focuses on off-policy algorithms. Some on-policy algorithms, such as A3C (Mnih et al., 2016), PPO (Schulman et al., 2017) or TRPO (Schulman et al., 2015) may be time discretization invariant with specific setups. This is out of the scope of our work and would require a separate study.

(Wang et al., 2015) also use a parameterization separating the value and advantage components of the Q -function. But contrary to (Baird, 1994)’s Advantage Updating, learning is still done in a standard way on the Q -function obtained from adding these two components. Thus this approach reparameterizes Q but does not change scalings and does not result in an invariant algorithm for small δt .

The problem studied here is a continuity effect quite distinct from multiscale RL approaches: indeed the issue arises even if there is only one timescale in the environment. Arguably, a small δt can be seen as a mismatch between the algorithm’s timescale and the physical system’s timescale, but the collapse of the Q function to the V function is an intrinsic mathematical phenomenon arising from time continuity.

Reinforcement learning has been studied from a mathematical perspective when time and space are both continuous, in connection with optimal control and the Hamilton–Jacobi–Bellman (HJB) equation (a PDE which characterizes the value function for continuous space-time). Explicit algorithms for continuous space-time can be found in (Doya, 2000; Munos & Bourgine, 1998) (see also the references therein). (Munos & Bourgine, 1998) use a grid approach to provably solve the HJB equation when discretization tends to 0 (assuming every state in the grid is visited a large number of times). However, the resulting algorithms are impractical (Doya, 2000) for larger-dimensional problems. (Doya, 2000) focusses on algorithms specific to the continuous space-time case, including advantage updating and modelling the time derivative of the environment.

Here on the other hand we focus on generic deep RL algorithms that can handle both discrete and continuous time and space, without collapsing in continuous time, thus being robust to arbitrary timesteps.

3. Near Continuous-Time Reinforcement Learning

Many reinforcement learning environments are not intrinsically time-discrete, but discretizations of an underlying continuous-time environment. For instance, many simulated control environments, such as the Mujoco environments (Lillicrap et al., 2015) or OpenAI Gym classic control environments (Brockman et al., 2016), are discretizations of continuous-time control problems. In simulated environments, the time discretization is fixed by the simulator, and is often used to approximate an underlying differential equation. In this case, the timestep may correspond to the number of frames generated by second. In real world environments, sensors and actuators have a fixed time precision: cameras can only capture a fixed amount of frames per second, and physical limitations prevent actuators from responding instantaneously. The quality of these components thus imposes a lower bound on the discretization timestep. As the timestep δt is largely a constraint imposed by computational resources, we would expect that decreasing δt would only improve the performance of RL agents (though it might make optimization harder). RL algorithms should, at least, be resilient to a change of δt , and should remain viable when $\delta t \rightarrow 0$. Besides, designing a time discretization invariant algorithm could alleviate tedious hyperparameteri-

zation by providing better defaults for time-horizon-related parameters.

We are thus interested in the behavior of RL algorithms in discretized environments, when the discretization timestep is small. We will refer to such environments as *near-continuous environments*. A formalized view of near-continuous environments is given below, along with δt -dependent definitions of return, discount factor and value functions, that converge to well defined continuous-time limits. The state-action value function is shown to collapse to the value function as δt goes to 0. Consequently there is no Q -learning in continuous time, foreshadowing problematic behavior of Q -learning with small timesteps.

3.1. Framework

Let $\mathcal{S} = \mathbb{R}^d$ be a set of states, and \mathcal{A} be a set of actions. Consider the continuous-time *Markov Decision Process* (MDP) defined by the differential equation

$$ds_t/dt = F(s_t, a_t) \quad (1)$$

where $F: \mathcal{S} \times \mathcal{A} \rightarrow \mathcal{S}$ describes the dynamics of the environment. The agent interacts with the environment through a deterministic policy function $\pi: \mathcal{S} \rightarrow \mathcal{A}$, so that $a_t = \pi(s_t)$. Actions can be discrete or continuous. For simplicity we assume here that both the dynamics and exploitation policy are deterministic;¹ the exploration policy will be random, but care must be taken to define proper random policies in continuous time, especially with discrete actions (Sec. 4.2).

For any timestep $\delta t > 0$, we can define an MDP $\mathcal{M}_{\delta t} = \langle \mathcal{S}, \mathcal{A}, T_{\delta t}, r_{\delta t}, \gamma_{\delta t} \rangle$ as a discretization of the continuous-time MDP with *time discretization* δt . The transition function of a state s is the state obtained when starting at $s_0 = s$ and maintaining $a_t = a$ constant for a time δt . This corresponds to an agent evolving in the continuous environment (1), but only making observations and choosing actions every δt . The rewards and decay factor are specified below. We call such an MDP $\mathcal{M}_{\delta t}$ *near-continuous*.

A necessary condition for robustness of an algorithm for near-continuous time MDPs is to remain viable when $\delta t \rightarrow 0$. Thus we will try to make sure the various quantities involved converge to meaningful limits when $\delta t \rightarrow 0$.

We give semi-formal statements below; the full statements, proofs, and technical assumptions (typically, differentiability assumptions) can be found in the supplementary material.

¹ We believe the results presented here hold more generally, assuming states follow a *stochastic* differential equation

$$ds = F(s, a)dt + \Sigma(s, a)dB_t \quad (2)$$

with B_t a multidimensional Brownian motion and Σ a covariance matrix. A formal treatment of SDEs is beyond the scope of this paper.

Return and discount factor. Suitable δt -dependent scalings of the discount factor $\gamma_{\delta t}$ and reward $r_{\delta t}$ are as follows. These definitions fit the discrete case when $\delta t = 1$, and provide well-defined, non-trivial returns and value functions when δt goes to 0.

For a continuous MDP and a continuous trajectory $\tau = (s_t, a_t)_t$, the return is defined as (Doya, 2000)

$$R(\tau) := \int_{t=0}^{\infty} \gamma^t r(s_t, a_t) dt. \quad (3)$$

A natural time discretization is obtained by defining the discretized return $R_{\delta t}$ of the MDP $\mathcal{M}_{\delta t}$ as

$$R_{\delta t}(\tau) := \sum_{k=0}^{\infty} \gamma^{k\delta t} r(s_{k\delta t}, a_{k\delta t}) \delta t \quad (4)$$

and the discretized return will correspond to the continuous-time return if we set the decay factor $\gamma_{\delta t}$ and rewards $r_{\delta t}$ of the discretized MDP $\mathcal{M}_{\delta t}$ to

$$\gamma_{\delta t} := \gamma^{\delta t}, \quad r_{\delta t} := \delta t \cdot r. \quad (5)$$

Physical time vs algorithmic time, time horizon. In near-continuous environments, there are two notions of time: the algorithmic time k (number of steps or actions taken), and the physical time t (time spent in the underlying continuous time environment), related via $t = k \cdot \delta t$.

The time horizon is, informally, the time range over which the agent optimizes its return. As a rule of thumb, the time horizon of an agent with discount factor γ is of order $\frac{1}{1-\gamma}$ steps; beyond that, the decay factor kicks in and the influence of further rewards becomes small.

The definition (5) of the decay factor $\gamma_{\delta t}$ in near-continuous environments keeps the time horizon constant in *physical* time, by making $\gamma_{\delta t}$ close to 1 in algorithmic time. Indeed, physical time horizon is δt times the algorithmic time horizon, namely

$$\frac{\delta t}{1 - \gamma_{\delta t}} = -\frac{1}{\log \gamma} + O(\delta t) \approx \frac{1}{1 - \gamma}, \quad (6)$$

which is thus stable when $\delta t \rightarrow 0$. On the other hand, if $\gamma_{\delta t}$ was left constant as δt goes to 0, the corresponding time horizon in physical time would be $\approx \frac{\delta t}{1-\gamma}$ which goes to 0 when δt goes to 0: such an agent would be increasingly short-sighted as $\delta t \rightarrow 0$.

In the following, we use the suitably-scaled decay factor (5) both for Deep Advantage Updating and for the classical deep Q -learning baselines.

Value function. The return (3) leads to the following continuous-time value function

$$V^\pi(s) = \mathbb{E}_{\tau \sim \pi} [R(\tau) \mid s_0 = s] \quad (7)$$

$$= \mathbb{E}_{\tau \sim \pi} \left[\int_0^\infty \gamma^t r(s_t, a_t) dt \mid s_0 = s \right]. \quad (8)$$

Meanwhile, the value function (in the ordinary sense) of the discrete MDP $\mathcal{M}_{\delta t}$ is

$$V_{\delta t}^\pi(s) = \mathbb{E}_{\tau \sim \pi} [R_{\delta t}(\tau) \mid s_0 = s] \quad (9)$$

$$= \mathbb{E}_{\tau \sim \pi} \left[\sum_{k=0}^{\infty} \gamma^{k\delta t} r(s_{k\delta t}, a_{k\delta t}) \delta t \mid s_0 = s \right] \quad (10)$$

which obeys the Bellman equation²

$$V_{\delta t}^\pi(s) = r(s, \pi(s)) \delta t + \gamma^{\delta t} \mathbb{E}_{s_{(k+1)\delta t} \mid s_{k\delta t} = s} V_{\delta t}^\pi(s_{(k+1)\delta t}) \quad (11)$$

When the timestep tends to 0, one converges to the other.

Theorem 1. *Under suitable smoothness assumptions, $V_{\delta t}^\pi(s)$ converges to $V^\pi(s)$ when $\delta t \rightarrow 0$.*

3.2. There is No Q -Function in Continuous Time

Contrary to the value function, the action-value function Q is ill-defined for continuous-time MDPs. More precisely, the Q -function collapses to the V -function when $\delta t \rightarrow 0$. In near continuous time, the effect of individual actions on the Q -function is of order $O(\delta t)$. This will make ranking of actions difficult, especially with an approximate Q -function. This argument appears informally in (Baird, 1994). Formally:

Theorem 2. *Under suitable smoothness assumptions, The action-value function of a near-continuous MDP is related to its value function via*

$$Q_{\delta t}^\pi(s, a) = V_{\delta t}^\pi(s) + O(\delta t) \quad (12)$$

when $\delta t \rightarrow 0$, for every (s, a) .

As a consequence, in exact continuous time, Q^π is equal to V^π : it does not bear *any* information on the ranking of actions, and thus cannot be used to select actions with higher returns. There is no continuous-time Q -learning.

Proof. The discrete-time Q -function of the MDP $\mathcal{M}_{\delta t}$ satisfies the Bellman equation

$$Q_{\delta t}^\pi(s, a) = r(s, a) \delta t + \gamma^{\delta t} \mathbb{E}_{s' \mid s, a} [V_{\delta t}^\pi(s')]. \quad (13)$$

² If the continuous MDP follows the dynamics (1), the limit of the Bellman equation (11) for $V_{\delta t}^\pi$ when $\delta t \rightarrow 0$ is the Hamilton–Jacobi–Bellman equation on V^π (Doya, 2000), namely, $r + \nabla_s V^\pi \cdot F = -\log(\gamma)V^\pi$.

The dynamics (1) of the environment yields

$$s' = s + F(s, a) \delta t + o(\delta t). \quad (14)$$

Assuming that $V_{\delta t}^\pi$ is continuously differentiable with respect to the state, and that its derivatives are uniformly bounded, we obtain,

$$V_{\delta t}^\pi(s') = V_{\delta t}^\pi(s) + \nabla_s V_{\delta t}^\pi(s) \cdot F(s, a) \delta t + o(\delta t) \quad (15)$$

$$= V_{\delta t}^\pi(s) + O(\delta t) \quad (16)$$

Expanding $V_{\delta t}^\pi(s')$ into $Q_{\delta t}^\pi$ yields

$$Q_{\delta t}^\pi(s, a) = r(s, a) \delta t + \gamma^{\delta t} (V_{\delta t}^\pi(s) + O(\delta t)) \quad (17)$$

$$= O(\delta t) + (1 + O(\delta t))(V_{\delta t}^\pi(s) + O(\delta t)) \quad (18)$$

$$= V_{\delta t}^\pi(s) + O(\delta t). \quad (19)$$

which ends the proof. \square

4. Reinforcement Learning with a Continuous-Time Limit

We now define a discrete algorithm with a well-defined continuous-time limit. It relies on three elements: defining and learning a quantity that still contains information on action rankings in the limit, using exploration methods with a meaningful limit, and scaling learning rates to induce well-behaved parameter trajectories when δt goes to 0.

4.1. Advantage Updating

As seen above, there is no continuous time limit to Q -learning, because Q^π becomes independent of actions and thus cannot be used to select actions. With small but nonzero δt , $Q_{\delta t}^\pi$ still depends on actions, and could still be used to choose actions. However, when approximating $Q_{\delta t}^\pi$, if the approximation error is much larger than $O(\delta t)$, this error dominates, the ranking of actions given by the approximated $Q_{\delta t}^\pi$ is likely to be erroneous.

To define an object which contains the same information on actions as $Q_{\delta t}^\pi$, but admits a learnable action-dependent limit, it is natural to define (Baird, 1994)

$$A_{\delta t}^\pi(s, a) := \frac{Q_{\delta t}^\pi(s, a) - V_{\delta t}^\pi(s)}{\delta t}, \quad (20)$$

a rescaled version of the advantage function, as the difference between $Q_{\delta t}^\pi(s, a)$ and $V_{\delta t}^\pi(s)$ is of order $O(\delta t)$. This amounts to splitting Q into value and advantage, and observing that these scale very differently when $\delta t \rightarrow 0$.

Contrary to the Q -function, this rescaled advantage function converges when $\delta t \rightarrow 0$ to a non-degenerate action-dependent quantity.

Theorem 3. *Under suitable smoothness assumptions, $A_{\delta t}^\pi(s, a)$ has a limit $A^\pi(s, a)$ when $\delta t \rightarrow 0$. The limit keeps information about actions: namely, if a policy π' strictly dominates π , then $A^\pi(s, \pi'(s)) > 0$ for some state s .*

Learning A^π . The discretized Q -function rewrites as

$$Q_{\delta t}^\pi(s, a) = V_{\delta t}^\pi(s) + \delta t A_{\delta t}^\pi(s, a). \quad (21)$$

A natural way to approximate $V_{\delta t}^\pi$ and $A_{\delta t}^\pi$ is to apply *Sarsa* or *Q*-learning to a reparameterized Q -function approximator

$$Q_\Theta(s, a) := V_\Theta(s) + \delta t A_\psi(s, a). \quad (22)$$

with $\Theta := (\theta, \psi)$. At initialization, if both V_θ and A_ψ are initialized independently of δt , this parameterization provides reasonable scaling of the contribution of actions versus states in Q . Our goal is for V_θ to approximate $V_{\delta t}^\pi$ and for A_ψ to approximate $A_{\delta t}^\pi$.

Still, this reparameterization does not, on its own, guarantee that A correctly approximates $A_{\delta t}^\pi$ if Q_Θ approximates $Q_{\delta t}^\pi$. Indeed, for any given pair (V_θ, A_ψ) , the pair $(V_\theta(s) - f(s), A_\psi(s, a) + f(s)/\delta t)$ (for an arbitrary f) yields the exact same function Q_Θ . This new A_ψ still defines the same ranking of actions, yet this phenomenon might cause numerical problems or instability of A_ψ when $\delta t \rightarrow 0$, and prevents direct interpretation of the learned A_ψ . To enforce identifiability of A_ψ , one must enforce the consistency equation

$$V_{\delta t}^\pi(s) = Q_{\delta t}^\pi(s, \pi(s)) \quad (23)$$

on the approximate A_ψ and V_θ . This translates to

$$A_\psi(s, \pi(s)) = 0. \quad (24)$$

With this additional constraint, if $Q_\Theta = Q_{\delta t}^\pi$, then $A_\psi = A_{\delta t}^\pi$ and $V_\theta = V_{\delta t}^\pi$: indeed

$$A_{\delta t}^\pi(s, a) = \frac{Q_{\delta t}^\pi(s, a) - V_{\delta t}^\pi(s)}{\delta t} \quad (25)$$

$$= \frac{Q_\Theta(s, a) - Q_\Theta(s, \pi(s))}{\delta t} = A_\psi(s, a). \quad (26)$$

In the spirit of (Wang et al., 2015), instead of directly parameterizing A_ψ , we define a parametric function \bar{A}_ψ (typically a neural network), and use \bar{A}_ψ to define A_ψ as

$$A_\psi(s, a) := \bar{A}_\psi(s, a) - \bar{A}_\psi(s, \pi(s)) \quad (27)$$

so that A_ψ directly verifies the consistency condition.

This approach will lead to δt -robust algorithms for approximating $A_{\delta t}^\pi$, from which a ranking of actions can be derived.

4.2. Timestep-Invariant Exploration

To obtain a timestep-invariant RL algorithm, a timestep-invariant exploration scheme is required. For *continuous* actions, (Lillicrap et al., 2015) already introduced such a scheme, by adding an *Ornstein–Uhlenbeck* (Uhlenbeck &

Ornstein, 1930) (OU) random process to the actions. Formally, this is defined as

$$\pi^{\text{explore}}(s_{k\delta t}, z_{k\delta t}) := \pi(s_{k\delta t}) + z_{k\delta t} \quad (28)$$

with $z_{k\delta t}$ the discretization of a continuous-time OU process,

$$dz_t = -z_t \kappa dt + \sigma dB_t. \quad (29)$$

where B_t is a brownian motion, κ a stiffness parameter and σ a noise scaling parameter. The discretized trajectories of z converge to nontrivial continuous-time trajectories, exhibiting Brownian behavior with a recall force towards 0.

This exploration can be extended to schemes of the form

$$a_{k\delta t} = \pi_{\delta t}^{\text{explore}}(s_{k\delta t}, z_{k\delta t}) \quad (30)$$

with $(z_{k\delta t})_{k \geq 0}$ a sequence of random variables independent from the a 's and s 's. A sufficient condition for this policy to admit a continuous-time limit is for the sequence $z_{k\delta t}$ to converge in law to a well-defined continuous stochastic process z_t as δt goes to 0.

Thus, for *discrete* actions we can obtain a consistent exploration scheme by taking $z_{\delta t}$ to be a discretization of an $(\#\mathcal{A})$ -dimensional continuous OU process, and setting

$$\pi^{\text{explore}}(s_{k\delta t}, z_{k\delta t}) := \operatorname{argmax}_a (A_\psi(s_{k\delta t}, a) + z_{k\delta t}[a]) \quad (31)$$

where $z_{k\delta t}[a]$ denotes the a -th component of $z_{k\delta t}$. Namely, we perturb the *advantage values* by a random process before selecting an action. The resulting scheme converges in continuous time to a nontrivial exploration scheme.

On the other hand, ε -greedy exploration is likely *not* to explore, i.e., to collapse to a deterministic policy, when δt goes to 0. Intuitively, with very small δt , changing the action at random every δt time step just averages out the randomness due to the law of large numbers. More precisely:

Theorem 4. *Consider a near-continuous MDP in which an agent selects an action according to an ε -greedy policy that mixes a deterministic exploitation policy π with an action taken from a noise policy $\pi^{\text{noise}}(a|s)$ with probability ε at each step. Then the agent's trajectories converge when $\delta t \rightarrow 0$ to the solutions of the deterministic equation*

$$ds_t/dt = (1 - \varepsilon)F(s_t, \pi(s_t)) + \varepsilon \mathbb{E}_{a \sim \pi^{\text{noise}}(a|s)} F(s_t, a) \quad (32)$$

4.3. Algorithms for Deep Advantage Updating

We learn V_θ and A_ψ via suitable variants of *Q*-learning for continuous and discrete action spaces. Namely, the true $A_{\delta t}^\pi$ and $V_{\delta t}^\pi$ of a near-continuous MDP with greedy exploitation policy $\pi(s) := \operatorname{argmax}_{a'} A_{\delta t}^\pi(s, a')$ are the unique solution

Algorithm 1 Deep Advantage Updating (Discrete actions)

Inputs:
 θ and ψ , parameters of V_θ and \bar{A}_ψ .

 π^{explore} and $\nu_{\delta t}$ defining an exploration policy.

 opt_V , opt_A , $\alpha^V \delta t$ and $\alpha^A \delta t$ optimizers and learning rates.

 \mathcal{D} , buffer of transitions (s, a, r, d, s') , with d the episode termination signal.

 δt and γ , time discretization and discount factor.

nb_epochs number of epochs.

nb_steps, number of steps per epoch.

 Observe initial state s^0
 $t \leftarrow 0$
for $e = 0, \text{nb_epochs}$ **do**
for $j = 1, \text{nb_steps}$ **do**
 $a^k \leftarrow \pi^{\text{explore}}(s^k, \nu_{\delta t}^k)$.

 Perform a^k and observe $(r^{k+1}, d^{k+1}, s^{k+1})$.

 Store $(s^k, a^k, r^{k+1}, d^{k+1}, s^{k+1})$ in \mathcal{D} .

 $k \leftarrow k + 1$
end for
for $k = 0, \text{nb_learn}$ **do**

 Sample a batch of N random transitions from \mathcal{D}
 $Q^i \leftarrow V_\theta(s^i) + \delta t (\bar{A}_\psi(s^i, a^i) - \max_{a'} \bar{A}_\psi(s^i, a'))$
 $\tilde{Q}^i \leftarrow r^i \delta t + (1 - d^i) \gamma^{\delta t} V_\theta(s'^i)$
 $\Delta\theta \leftarrow \frac{1}{N} \sum_{i=1}^N \frac{(Q^i - \tilde{Q}^i) \partial_\theta V_\theta(s^i)}{\delta t}$
 $\Delta\psi \leftarrow \frac{1}{N} \sum_{i=1}^N \frac{(Q^i - \tilde{Q}^i) \partial_\psi (\bar{A}_\psi(s^i, a^i) - \max_{a'} \bar{A}_\psi(s^i, a'))}{\delta t}$

 Update θ with opt_1 , $\Delta\theta$ and learning rate $\alpha^V \delta t$.

 Update ψ with opt_2 , $\Delta\psi$ and learning rate $\alpha^A \delta t$.

end for
end for

to the Bellman and consistency equations

$$V_{\delta t}^\pi(s) + \delta t A_{\delta t}^\pi(s, a) = r \delta t + \gamma^{\delta t} \mathbb{E}_{s'} V_{\delta t}^\pi(s') \quad (33)$$

$$A_{\delta t}^\pi(s, \pi(s)) = 0. \quad (34)$$

 as seen in 4.1. Thus V_θ and A_ψ are trained to approximately solve these equations.

 Maximization over actions for π is implemented exactly for discrete actions, and, for continuous actions, approximated by a policy neural network $\pi_\phi(s)$ trained to maximize $A_\psi(s, \pi_\phi(s))$, similarly to (Lillicrap et al., 2015).

 Eq. (34) is directly verified by A_ψ , owing to the reparametrization $A_\psi(s, a) = \bar{A}_\psi(s, a) - \bar{A}_\psi(s, \pi(s))$, described in 4.1. To approximately verify (33), the corresponding squared Bellman residual is minimized by an approximate gradient descent. The update equations when learning from a transition (s, a, r, s') , either from an exploratory

trajectory or from a replay buffer (Mnih et al., 2015), are

$$\delta Q_{\delta t} \leftarrow A_\psi(s, a) \delta t - (r \delta t + \gamma^{\delta t} V_\theta(s') - V_\theta(s)) \quad (35)$$

$$\theta_{\delta t} \leftarrow \theta_{\delta t} + \eta_{\delta t}^V \partial_\theta V_\theta(s) \frac{\delta Q_{\delta t}}{\delta t} \quad (36)$$

$$\psi_{\delta t} \leftarrow \psi_{\delta t} + \eta_{\delta t}^A \partial_\psi A_\psi(s, a) \frac{\delta Q_{\delta t}}{\delta t}. \quad (37)$$

 where the η 's are learning rates. Appropriate scalings for the learning rates $\eta_{\delta t}^V$ and $\eta_{\delta t}^A$ in terms of δt to obtain a well defined continuous limit are derived next.

4.4. Scaling the Learning Rates

 For the algorithm to admit a continuous-time limit, the discrete-time trajectories of parameters must converge to well-defined trajectories as δt goes to 0. This in turn imposes precise conditions on the scalings of the learning rates.

 Informally, in the parameter updates (35)–(37), the quantity $\delta Q_{\delta t}$ is of order $O(\delta t)$, because $s' = s + O(\delta t)$ in a near-continuous system. Therefore, $\delta Q_{\delta t} / \delta t$ is $O(1)$, so that the gradients used to update θ and ψ are $O(1)$. Therefore, if the learning rates are of order δt , one would expect the parameters θ and ψ to change by $O(\delta t)$ in each time interval δt , thus hopefully converging to smooth continuous-time trajectories. The next theorem formally confirms that learning rates of order δt are the only possibility.

Theorem 5. *Let (s_t, a_t) be some exploration trajectory in a near-continuous MDP. Set the learning rates to $\eta_{\delta t}^V = \alpha^V \delta t^\beta$ and $\eta^A = \alpha^A \delta t^\beta$ for some $\beta \geq 0$, and learn the parameters θ and ψ by iterating (35)–(37) along the trajectory (s_t, a_t) . Then, when $\delta t \rightarrow 0$:*

- If $\beta = 1$ the discrete parameter trajectories converge to continuous parameter trajectories.
- If $\beta > 1$ the parameters stay at their initial values.
- If $\beta < 1$, the parameters can reach infinity in arbitrarily small physical time.

 The resulting algorithm with suitable scalings, *Deep Advantage Updating* (DAU), is specified in Alg. 1 for discrete actions, and in the Supplementary for continuous actions.

5. Experiments

The experiments provided here are specifically aimed at showing that the proposed method, DAU, works efficiently over a wide range of time discretizations, without specific tuning, while standard deep Q-learning approaches do not. DAU is compared to DDPG for continuous actions and to DQN for discrete actions. As mentioned earlier, we do not study the time discretization invariance of on-policy methods (A3C, PPO, TRPO...).

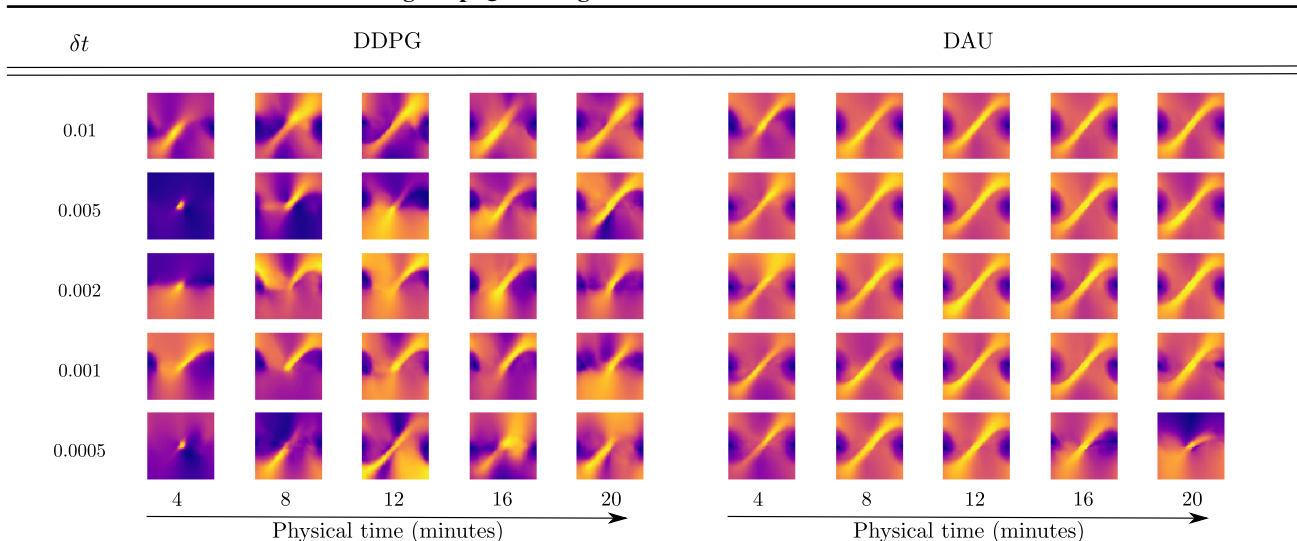


Figure 1. Value functions obtained by DDPG (unscaled version) and DAU at different instants in physical time of training on the pendulum swing-up environment. Each image represents the learnt value function (the x -axis is the angle, and the y -axis the angular velocity). The lighter the pixel, the higher the value.

In all setups, we use the algorithms described in Alg. 1 and Supplementary Alg. 1. The variants of DDPG and DQN used are described in the Supplementary, as well as all hyperparameters. We tested two different setups for DDPG and DQN. In one, we scaled the discount factor (to avoid shortsightedness with small δt), but left all other hyperparameters constant across time discretizations. In the other, we used the properly rescaled discount factor and reward from Eq. (5), as well as $O(\delta t)$ learning rates for RMSProp. The first variant yields slightly better results, and is presented here, with the second variant in the Supplementary. For all setups, quantitative results are averaged over five runs.

Let us stress that the quantities plotted are rescaled to make comparison possible across different timesteps. For example, returns are given in terms of the discretized return $R_{\delta t}$ as defined in (4),³ and, most notably, time elapsed is always given in *physical* time, i.e., the amount of time that the agent spent interacting with the environment (this is not the number of steps).

Qualitative experiments: Visualizing policies and values. To provide qualitative results, and check robustness to time discretization both in terms of returns and in terms of convergence of the approximate value function and policies, we first provide results on the simple pendulum environment from the OpenAI Gym classic control suite. The state space is of dimension 2. We visualize both the learnt value and

³This mostly amounts to scaling rewards by a factor δt when this scaling is not naturally done in the environment. Environment-specific details are given in the Supplementary.

policy functions by plotting, for each point of the phase diagram $(\theta, \dot{\theta})$, its value and policy. The results are presented in Fig. 1 (value function) and Figs. 1, 2, 3 in Supplementary.

We plot the learnt policy at several instants in physical time during training, for various time discretizations δt , for both DAU and DDPG. With DAU, the agent’s policy and value function quickly converge for every time discretization without specific tuning. On the contrary, with DDPG, learning of both value function and policy vary greatly from one discretization to another.

Quantitative experiments. We benchmark DAU against DDPG on classic control benchmarks: Pendulum, Cartpole, BipedalWalker, Ant, and Half-Cheetah environments from OpenAI Gym. On Pendulum, Bipedal Walker and Ant, DAU is quite robust to variations of δt and displays reasonable performance in all cases. On the other hand, DDPG’s performance varies with δt ; performance either degrades as δt decreases (Ant, Cheetah), or becomes more variable as learning progresses (Pendulum) for small δt . On Cartpole, noise dominates, making interpretation difficult. On Half-Cheetah, DAU is not clearly invariant to time discretization. This could be explained by the multiple suboptimal regimes that coexist in the Half-Cheetah environment (walking on the head, walking on the back), which create discontinuities in the value function (see Discussion).

6. Discussion

The method derived in this work is theoretically invariant to time discretization, and indeed seems to yield improved

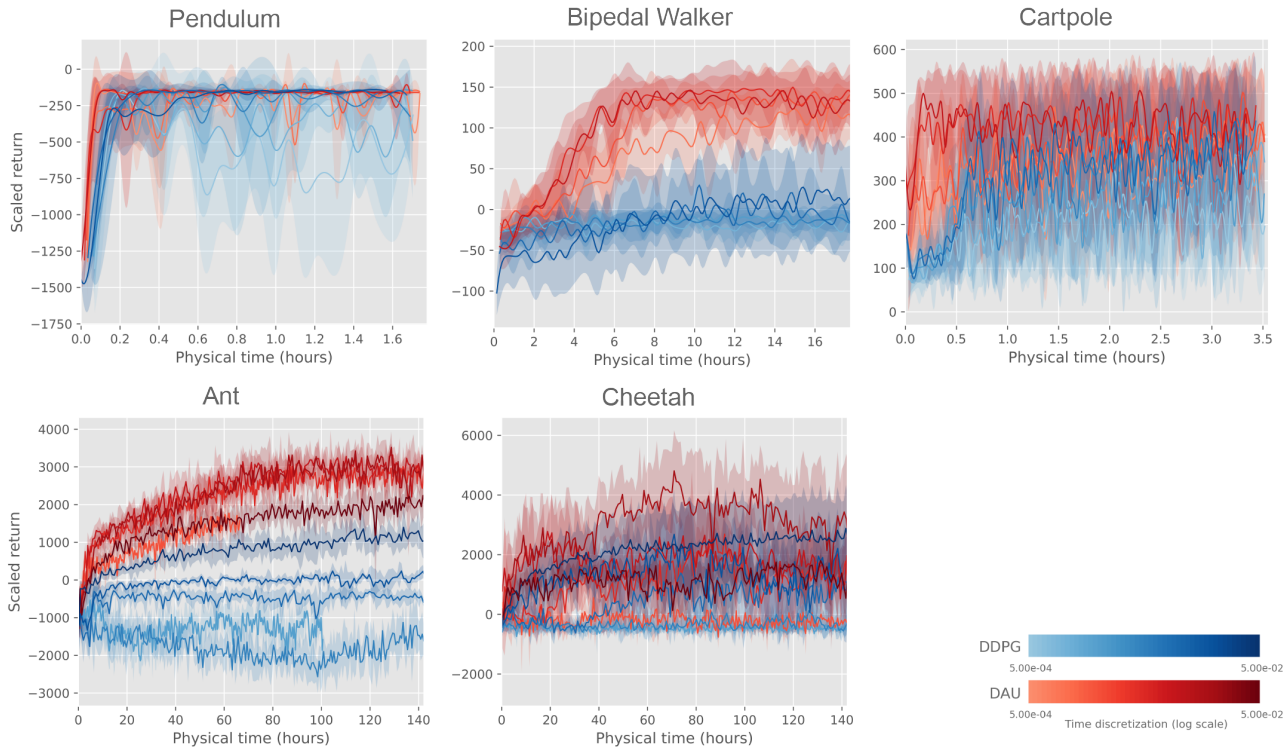


Figure 2. Learning curves for DAU and DDPG on classic control benchmarks for various time discretization δt : Scaled return as a function of the physical time spent in the environment.

timestep robustness on various environments, e.g., simple locomotion tasks. However, on some environments there is still room for improvement. We discuss some of the issues that could explain this theoretical/practical discrepancy.

Note that Alg. 1 requires knowledge of the timestep δt . In most environments, this is readily available, or even directly set by the practitioner: depending on the environment it is given by the frame rate, the maximum frequency of actuators or observation acquisition, the timestep of a physics simulator, etc.

Smoothness of the value function. In our proofs, V^π is assumed to be continuously differentiable. This hypothesis is not always satisfied in practice. For instance, in the pendulum swing-up environment, depending on initial position and momentum, the optimal policy may need to oscillate before reaching the target state. The optimal value function is discontinuous at the boundary between states where oscillations are needed and those where they are not. This results in non-infinitesimal advantages for actions on the boundary. In such environments where a given policy has different regimes depending on the initial state, the continuous-time analysis only holds almost-everywhere.

Memory buffer size. Thm. 5 is stated for transitions sampled sequentially from a fixed trajectory. In practice,

transitions are sampled from a memory replay buffer, to prevent excessive correlations. We used a fixed-size circular buffer, filled with samples from a single growing exploratory trajectory. In our experiments, the same buffer size was used for all time discretizations. Thus the physical-time freshness of samples in the buffer varies with the time discretization, and in the strictest sense using a fixed-size buffer breaks timestep invariance. A memory-intensive option would be to use a buffer of size $\frac{1}{\delta t}$ (fixed memory in physical time).

Near-continuous reinforcement learning and RMSProp. RMSProp (Tieleman & Hinton, 2012) divides gradient steps by the square root of a moving average estimate of the second moment of gradients. This may interact with the learning rate scaling discussed above. In deterministic environments, gradients typically scale as $O(1)$ in terms of δt , as seen in (37). In that case, RMSProp preconditioning has no effect on the suitable order of magnitude for learning rates. However, in near continuous *stochastic* environments (Eq. 2), variance of $\delta Q_{\delta t} / \delta t$ and of the gradients typically scales as $O(1/\delta t)$. With a fixed batch size, RMSProp will multiply gradients by a factor $O(\sqrt{\delta t})$. In that case, learning rates need only be scaled as $\sqrt{\delta t}$ instead of δt .

More generally, the continuous-time analysis should in principle be repeated for every component of a system. For instance, if a recurrent model is used to handle state memory

or partial observability, care should be taken that the model is able to maintain memory for a non-infinitesimal physical time when $\delta t \rightarrow 0$ (see e.g. Tallec & Ollivier 2018).

7. Conclusion

Q-learning methods have been found to fail to learn with small time steps, both theoretically and empirically. A theoretical analysis help in building a practical off-policy deep RL algorithm with better robustness to time discretization. This robustness is confirmed empirically.

Acknowledgments

We would like to thank Harsh Satija and Joelle Pineau for their useful remarks and comments.

References

- Baird, L. C. Reinforcement learning in continuous time: Advantage updating. In *Neural Networks, 1994. IEEE World Congress on Computational Intelligence., 1994 IEEE International Conference on*, volume 4, pp. 2448–2453. IEEE, 1994.
- Brockman, G., Cheung, V., Pettersson, L., Schneider, J., Schulman, J., Tang, J., and Zaremba, W. Openai gym, 2016.
- Doya, K. Reinforcement learning in continuous time and space. *Neural computation*, 12(1):219–245, 2000.
- Henderson, P., Islam, R., Bachman, P., Pineau, J., Precup, D., and Meger, D. Deep reinforcement learning that matters. *CoRR*, abs/1709.06560, 2017. URL <http://arxiv.org/abs/1709.06560>.
- Lillicrap, T. P., Hunt, J. J., Pritzel, A., Heess, N., Erez, T., Tassa, Y., Silver, D., and Wierstra, D. Continuous control with deep reinforcement learning. *CoRR*, abs/1509.02971, 2015. URL <http://arxiv.org/abs/1509.02971>.
- Mnih, V., Kavukcuoglu, K., Silver, D., Rusu, A. A., Veness, J., Bellemare, M. G., Graves, A., Riedmiller, M., Fidjeland, A. K., Ostrovski, G., et al. Human-level control through deep reinforcement learning. *Nature*, 518(7540): 529, 2015.
- Mnih, V., Badia, A. P., Mirza, M., Graves, A., Lillicrap, T., Harley, T., Silver, D., and Kavukcuoglu, K. Asynchronous methods for deep reinforcement learning. In *International conference on machine learning*, pp. 1928–1937, 2016.
- Munos, R. and Bourgin, P. Reinforcement learning for continuous stochastic control problems. In *Advances in neural information processing systems*, pp. 1029–1035, 1998.
- OpenAI. Learning dexterous in-hand manipulation. *CoRR*, abs/1808.00177, 2018a. URL <http://arxiv.org/abs/1808.00177>.
- OpenAI. Openai five. <https://blog.openai.com/openai-five/>, 2018b.
- Schulman, J., Levine, S., Abbeel, P., Jordan, M., and Moritz, P. Trust region policy optimization. In *International Conference on Machine Learning*, pp. 1889–1897, 2015.
- Schulman, J., Wolski, F., Dhariwal, P., Radford, A., and Klimov, O. Proximal policy optimization algorithms. *arXiv preprint arXiv:1707.06347*, 2017.
- Silver, D., Hubert, T., Schrittwieser, J., Antonoglou, I., Lai, M., Guez, A., Lanctot, M., Sifre, L., Kumaran, D., Graepel, T., et al. Mastering chess and shogi by self-play with a general reinforcement learning algorithm. *arXiv preprint arXiv:1712.01815*, 2017.
- Tallec, C. and Ollivier, Y. Can recurrent neural networks warp time? *arXiv preprint arXiv:1804.11188*, 2018.
- Tieleman, T. and Hinton, G. Lecture 6.5-rmsprop: Divide the gradient by a running average of its recent magnitude. *COURSERA: Neural networks for machine learning*, 4 (2):26–31, 2012.
- Uhlenbeck, G. E. and Ornstein, L. S. On the theory of the Brownian motion. *Physical review*, 36(5):823, 1930.
- Wang, Z., Schaul, T., Hessel, M., Van Hasselt, H., Lanctot, M., and De Freitas, N. Dueling network architectures for deep reinforcement learning. *arXiv preprint arXiv:1511.06581*, 2015.
- Zhang, A., Wu, Y., and Pineau, J. Natural environment benchmarks for reinforcement learning. *CoRR*, abs/1811.06032, 2018. URL <http://arxiv.org/abs/1811.06032>.

A. Proofs

We now give proofs for all the results presented in the paper. Most proofs follow standard patterns from calculus and numerical schemes for differential equations, except for Theorem 8, which uses an argument specific to reinforcement learning to prove that the continuous-time advantage function contains all the necessary information for policy improvement.

The first result presented is a proof of convergence for discretized trajectories.

Lemma 1. *Let $F: \mathcal{S} \times \mathcal{A} \rightarrow \mathbb{R}^n$ and $\pi: \mathcal{S} \rightarrow \mathcal{A}$ be the dynamic and policy functions. Assume that, for any a , $s \rightarrow F(s, a)$ and $s \rightarrow F(s, \pi(s))$ are \mathcal{C}^1 , bounded and K -lipschitz. For a given s_0 , define the trajectory $(s_t)_{t \geq 0}$ as the unique solution of the differential equation*

$$\frac{ds_t}{dt} = F(s_t, \pi(s_t)). \quad (38)$$

For any $\delta t > 0$, define the discretized trajectory $(s_{\delta t}^k)_k$ which amounts to maintaining each action for a time interval δt ; it is defined by induction as $s_{\delta t}^0 = s_0$, $s_{\delta t}^{k+1}$ is the value at time δt of the unique solution of

$$\frac{d\tilde{s}_t}{dt} = F(\tilde{s}_t, \pi(s_{\delta t}^k)) \quad (39)$$

with initial point $s_{\delta t}^k$. Then, there exists $C > 0$ such that, for every $t \geq 0$

$$\|s_t - s_{\delta t}^{\lfloor t/\delta t \rfloor}\| \leq \delta t \frac{C}{K} e^{Kt}. \quad (40)$$

Therefore, discretized trajectories converge pointwise to continuous trajectories.

Proof. The proof mostly follows the classical argument for convergence of the Euler scheme for differential equations. For any k , define

$$e_{\delta t}^k = \|s_{\delta t}^k - s_{\delta t k}\|. \quad (41)$$

Let \tilde{s}_t be the solution of Eq. (101) with initial state $s_{\delta t}^k$. This \tilde{s}_t is \mathcal{C}^2 on $[0, \delta t]$. Consequently, the Taylor integral formula gives

$$s_{\delta t}^{k+1} = s_{\delta t}^k + F(s_{\delta t}^k, \pi(s_{\delta t}^k))\delta t + \int_0^{\delta t} (\delta t - t) \frac{d^2 \tilde{s}_t}{dt^2} dt \quad (42)$$

$$s_{\delta t(k+1)} = s_{\delta t k} + F(s_{\delta t k}, \pi(s_{\delta t k}))\delta t + \int_0^{\delta t} (\delta t - t) \frac{d^2 s_{t+\delta t k}}{dt^2} dt. \quad (43)$$

Now, both $d^2 s_t/dt^2$ and $d^2 \tilde{s}_t/dt^2$ are uniformly bounded, by boundedness and Lipschitzness of $s \rightarrow F(s, \pi(s))$ and

$s \rightarrow F(s, \pi(s_{\delta t}^k))$. Consequently, there exists C such that

$$e_{\delta t}^{k+1} \leq \|s_{\delta t}^k - s_{\delta t k}\| + \|F(s_{\delta t}^k, \pi(s_{\delta t}^k)) - F(s_{\delta t k}, \pi(s_{\delta t k}))\|\delta t + C\delta t^2 \quad (44)$$

$$\leq (1 + K\delta t)e_{\delta t}^k + C\delta t^2. \quad (45)$$

Now, it is easy to prove by induction that

$$e_{\delta t}^k \leq (1 + K\delta t)^k (e_{\delta t}^0 + \frac{C}{K}\delta t) - \frac{C}{K}\delta t. \quad (46)$$

As $e_{\delta t}^0 = 0$, this translates to

$$e_{\delta t}^k \leq ((1 + K\delta t)^k - 1)\delta t \frac{C}{K} \quad (47)$$

$$\leq (e^{K\delta t k} - 1)\delta t \frac{C}{K}. \quad (48)$$

Consequently,

$$e_{\delta t}^{\lfloor t/\delta t \rfloor} \leq (e^{K(t+\delta t)} - 1)\delta t \frac{C}{K}. \quad (49)$$

Finally, by boundedness, of $s \rightarrow F(s, \pi(s))$, there exists C' such that

$$\|s_{\delta t \lfloor t/\delta t \rfloor} - s_t\| \leq \delta t C'. \quad (50)$$

Combining Eq. (50) with Eq. (49), one can find C'' such that

$$\|s_t - s_{\delta t}^{\lfloor t/\delta t \rfloor}\| \leq \delta t \frac{C''}{K} e^{Kt}. \quad (51)$$

□

In what follows, we assume that the continuous-time reward function $r: \mathcal{S} \times \mathcal{A} \rightarrow \mathbb{R}$ is bounded, to ensure existence of V^π and $V_{\delta t}^\pi$ for all δt .

Theorem 6. *Assume that $r: \mathcal{S} \times \mathcal{A} \rightarrow \mathbb{R}$ is bounded, and that $s \rightarrow r(s, \pi(s))$ is L_r -Lipschitz continuous, then for all $s \in \mathcal{S}$, one has $V_{\delta t}^\pi(s) = V^\pi(s) + o(1)$ when $\delta t \rightarrow 0$.*

Proof. We use the notation $\tilde{r}(s) = r(s, \pi(s))$. Let $\tilde{s}_{\delta t}^t := s_{\delta t}^{\lfloor t/\delta t \rfloor}$. We have:

$$V_{\delta t}^\pi(s) = \int_t^\infty \gamma^t \tilde{r}(\tilde{s}_{\delta t}^t) dt + O(\delta t) \quad (52)$$

Indeed:

$$V_{\delta t}^\pi(s) = \sum_{k=0}^{\infty} \gamma^{k\delta t} \tilde{r}(s_{\delta t}^k) \delta t \quad (53)$$

$$= \sum_{k=0}^{\infty} \gamma^{k\delta t} \int_{u=k}^{k+1} \tilde{r}(\tilde{s}_{\delta t}^{u\delta t}) du \quad (54)$$

$$= \sum_{k=0}^{\infty} \frac{\delta t \log \gamma}{\gamma^{\delta t} - 1} \int_{u=k}^{k+1} \gamma^{u\delta t} \tilde{r}(\tilde{s}_{\delta t}^{u\delta t}) du \quad (55)$$

$$= \frac{\delta t \log \gamma}{\gamma^{\delta t} - 1} \int_{t=0}^{\infty} \gamma^t \tilde{r}(\tilde{s}_{\delta t}^t) dt \quad (56)$$

$$(57)$$

But:

$$\frac{\delta t \log \gamma}{\gamma^{\delta t} - 1} = \frac{\delta t \log \gamma}{\delta t \log \gamma + O(\delta t^2)} \quad (58)$$

$$= 1 + O(\delta t) \quad (59)$$

$$(60)$$

Therefore:

$$V_{\delta t}^{\pi}(s) = \int_t^T \gamma^t \tilde{r}(\tilde{s}_{\delta t}^t) dt + O(\delta t) \quad (61)$$

We now have, for any $T > 0$,

$$|V_{\delta t}^{\pi}(s) - V^{\pi}(s)| = \left| \int_{t=0}^{\infty} \gamma^t (\tilde{r}(\tilde{s}_{\delta t}^t) - \tilde{r}(s_t)) dt \right| + O(\delta t) \quad (62)$$

$$= \left| \int_{t=0}^T \gamma^t (\tilde{r}(\tilde{s}_{\delta t}^t) - \tilde{r}(s_t)) dt \right| \quad (63)$$

$$+ \left| \int_{t=T}^{\infty} \gamma^t (\tilde{r}(\tilde{s}_{\delta t}^t) - \tilde{r}(s_t)) dt \right| + O(\delta t) \quad (64)$$

The second term can be bounded by the supremum of the reward:

$$\left| \int_{t=T}^{\infty} \gamma^t (\tilde{r}(\tilde{s}_{\delta t}^t) - \tilde{r}(s_t)) dt \right| \leq 2 \frac{\|r\|_{\infty}}{\log(\frac{1}{\gamma})} \gamma^T \quad (65)$$

The first term can be bounded by using Lemma. 1:

$$\left| \int_{t=0}^T \gamma^t (\tilde{r}(\tilde{s}_{\delta t}^t) - \tilde{r}(s_t)) dt \right| \leq \int_{t=0}^T \gamma^t L_r \|s_t - \tilde{s}_{\delta t}^t\| dt \quad (66)$$

$$\leq \int_{t=0}^T L_r \frac{C \delta t}{K} \exp((K + \log \gamma)t) dt \quad (67)$$

$$\leq \frac{L_r C}{K(K + \log \gamma)} \exp((K + \log \gamma)T) \delta t \quad (68)$$

Let us set $T := -\frac{1}{K} \log(\delta t)$. By plugging into Eq. (65), we have:

$$\left| \int_{t=T}^{\infty} \gamma^t (\tilde{r}(\tilde{s}_{\delta t}^t) - \tilde{r}(s_t)) dt \right| = O(\delta t^{-\log \gamma}) = o(1). \quad (69)$$

By plugging T into equation (68), we have:

$$\left| \int_{t=0}^T \gamma^t (\tilde{r}(\tilde{s}_{\delta t}^t) - \tilde{r}(s_t)) dt \right| = O(\delta t^{-\frac{\log \gamma}{K}}) = o(1), \quad (70)$$

yielding our result. \square

For the following proof, we further assume that both V^{π} and $V_{\delta t}^{\pi}$ are continuously differentiable, and that the gradient and Hessian of $V_{\delta t}^{\pi}$ w.r.t. s are uniformly bounded in both s and δt . We also assume convergence of $\partial_s V_{\delta t}^{\pi}(s)$ to $\partial_s V^{\pi}(s)$ for all s .

Theorem 7. *Under the hypothesis above, there exists $A^{\pi} : \mathcal{S} \rightarrow \mathbb{R}$ such that $A_{\delta t}^{\pi}$ converges pointwise to A^{π} as δt goes to 0. Besides,*

$$A^{\pi}(s, a) = r(s, a) + \partial_s V^{\pi}(s) F(s, a) + \log \gamma V^{\pi}(s). \quad (71)$$

Proof. Denote $\tilde{s}_{\delta t}^t(s_0)$ the evaluation at instant t of the solution of $d\tilde{s}_t/dt = F(\tilde{s}_t, \pi(s_0))$ with starting point s_0 .

The Bellman equation on $Q_{\delta t}^{\pi}$ yields

$$Q_{\delta t}^{\pi}(s, a) = r(s, a) \delta t + \gamma^{\delta t} V_{\delta t}^{\pi}(\tilde{s}_{\delta t}^{\delta t}(s)). \quad (72)$$

For all s , a first-order Taylor expansion yields

$$\tilde{s}_{\delta t}^{\delta t}(s) = s + F(s, a) \delta t + O(\delta t^2) \quad (73)$$

where the constant in $O()$ is uniformly bounded thanks to the assumptions on the Hessian. Thus, by uniform boundedness of the Hessian of $V_{\delta t}^{\pi}$,⁴

$$Q_{\delta t}^{\pi}(s, a) = r(s, a) \delta t + (1 + \ln(\gamma) \delta t + O(\delta t^2)) (V_{\delta t}^{\pi}(s) + \delta t \partial_s V_{\delta t}^{\pi}(s) F(s, a) + O(\delta t^2)). \quad (74)$$

Now, this yields

$$A_{\delta t}^{\pi}(s, a) = r(s, a) + \ln(\gamma) V_{\delta t}^{\pi}(s) + \partial_s V_{\delta t}^{\pi}(s) F(s, a) + O(\delta t), \quad (75)$$

and using the convergence of $V_{\delta t}^{\pi}(s)$ to $V^{\pi}(s)$ (Thm. 6) and $\partial_s V_{\delta t}^{\pi}(s)$ to $\partial_s V^{\pi}(s)$ (hypothesis) yields the result with

$$A^{\pi}(s, a) = r(s, a) + \ln(\gamma) V^{\pi}(s) + \partial_s V^{\pi}(s) F(s, a). \quad (76)$$

\square

We now show that policy improvement works with the continuous time advantage function, i.e.

Theorem 8. *Let π and π' be two policies such that both $s \rightarrow r(s, \pi(s))$ and $s \rightarrow r(s, \pi'(s))$ are continuous. Assume that both V^{π} and $V^{\pi'}$ are continuously differentiable. Define the advantage function for policies π and π' as in Eq. (76).*

If for all s , $A^{\pi}(s, \pi'(s)) \geq 0$, then for all s , $V^{\pi}(s) \leq V^{\pi'}(s)$. Moreover, if for all s , $V^{\pi'}(s) > V^{\pi}(s)$, then there exists s' such that $A^{\pi}(s', \pi'(s')) > 0$.

⁴ Without boundedness of the Hessian, we cannot write the second order Taylor expansion of $V_{\delta t}^{\pi}(\tilde{s}_{\delta t}^{\delta t}(s))$ in term of δt . \square

Proof. Let $(s_t)_{t \geq 0}$ be a trajectory sampled from π' i.e. solution of the equation

$$ds_t/dt = F(s_t, \pi'(s_t)) \quad (77)$$

with initial condition $s_0 = s$.

Define

$$B(T) = \int_{t=0}^T \gamma^t r(s_t, \pi'(s_t)) dt + \gamma^T V^\pi(s_T). \quad (78)$$

This function is continuously differentiable, and its derivative is

$$\dot{B}(T) = \gamma^T r(s_T, \pi'(s_T)) \quad (79)$$

$$+ \gamma^T \partial_s V^\pi(s) F(s, \pi'(s)) + \gamma^T \ln(\gamma) V^\pi(s_T) \quad (80)$$

$$= \gamma^T A^\pi(s_T, \pi'(s_T)) \quad (81)$$

$$\geq 0. \quad (82)$$

Thus B is increasing, and $B(0) = V^\pi(s)$, $\lim_{T \rightarrow \infty} B(t) = V^{\pi'}(s)$. Consequently, $V^\pi(s) \leq V^{\pi'}(s)$. Furthermore, if $V^\pi(s) < V^{\pi'}(s)$, then there exists T_0 such that $\dot{B}(T_0) > 0$ (otherwise B is constant), and $A^\pi(s_{T_0}, \pi'(s_{T_0})) > 0$. \square

Theorem 9. Let $\mathcal{A} = \mathbb{R}^A$ be the action space, and let $\mathcal{P}_1 = \mathbb{R}^{P_1}$ and $\mathcal{P}_2 = \mathbb{R}^{P_2}$ be parameter spaces. Let $A: \mathcal{P}_1 \times \mathcal{S} \times \mathcal{A} \rightarrow \mathbb{R}$ and $V: \mathcal{P}_2 \times \mathcal{S} \rightarrow \mathbb{R}$ be \mathcal{C}^2 function approximators with bounded gradients and Hessians. Let $(a_t)_{t \geq 0}$ be a \mathcal{C}^1 exploratory action trajectory and $(s_t)_{t \geq 0}$ the resulting state trajectory, when starting from s_0 and following $ds_t/dt = F(s_t, a_t)$. Let $\theta_{\delta t}^k$ and $\psi_{\delta t}^k$ be the discrete parameter trajectories resulting from the gradient descent steps in the main text, with learning rates $\eta^V = \alpha^V \delta t^\beta$ and $\eta^A = \alpha^A \delta t^\beta$ for some $\beta \geq 0$. Then,

- If $\beta = 1$ the discrete parameter trajectories converge to continuous parameter trajectories as δt goes to 0.
- If $\beta > 1$, parameter trajectories become stationary as δt goes to 0.
- If $\beta < 1$, parameters can grow arbitrarily large after an arbitrarily small physical time when δt goes to 0.

Proof. Let $(s_t, a_t)_{t \geq 0}$ be the trajectory on which parameters are learnt. To simplify notations, define

$$A_\psi(s, a) = \bar{A}_\psi(s, a) - \bar{A}_\psi(s, \pi(s)). \quad (83)$$

Define F as

$$F^\theta(\theta, \psi, s, a) = \alpha^V (r(s, a) + \ln(\gamma) V_\theta(s) + \partial_s V_\theta(s) F(s, a) - A_\psi(s, a)) \partial_\theta V_\theta(s) \quad (84)$$

$$F^\psi(\theta, \psi, s, a) = \alpha^A (r(s, a) + \ln(\gamma) V_\theta(s) + \partial_s V_\theta(s) F(s, a) - A_\psi(s, a)) \partial_\psi A_\psi(s, a). \quad (85)$$

From the bounded Hessians and Gradients hypothesis, V , A , $\partial_s V$, $\partial_\theta V$ and $\partial_\psi A$ are uniformly Lipschitz continuous in θ and ψ , thus F is Lipschitz continuous.

The discrete equations for parameters updates with learning rates $\alpha^V \delta t^\beta$ and $\alpha^A \delta t^\beta$ are

$$\delta Q = r(s_{k\delta t}, a_{k\delta t}) \delta t + \gamma^{\delta t} V_{\theta_{\delta t}^k}(s_{(k+1)\delta t}) - V_{\theta_{\delta t}^k}(s_{k\delta t}) - A_\psi(s_{k\delta t}, a_{k\delta t}) \quad (86)$$

$$\theta_{\delta t}^{k+1} = \theta_{\delta t}^k + \alpha^V \delta t^\beta \frac{\delta Q}{\delta t} \partial_\theta V_{\theta_{\delta t}^k}(s_{k\delta t}) \quad (87)$$

$$\psi_{\delta t}^{k+1} = \psi_{\delta t}^k + \alpha^A \delta t^\beta \frac{\delta Q}{\delta t} \partial_\psi A_{\theta_{\delta t}^k}(s_{k\delta t}, a_{k\delta t}) \quad (88)$$

Under uniform boundedness of the Hessian of $s \mapsto V_\theta(s)$, one can show

$$\begin{pmatrix} \theta_{\delta t}^{k+1} \\ \psi_{\delta t}^{k+1} \end{pmatrix} = \begin{pmatrix} \theta_{\delta t}^k \\ \psi_{\delta t}^k \end{pmatrix} + \delta t^\beta F(\theta_{\delta t}^k, \psi_{\delta t}^k, s_{k\delta t}, a_{k\delta t}) + O(\delta t^\beta \delta t), \quad (89)$$

with a O independent of k . With the additional hypothesis that the gradient of $(s, a) \rightarrow \bar{A}_\psi(s, a)$ is uniformly bounded, we have

- For $\beta = 1$, a proof scheme identical to that of Thm. 1 shows that discrete trajectories converge pointwise to continuous trajectories defined by the differential equation

$$\frac{d}{dt} \begin{pmatrix} \theta_t \\ \psi_t \end{pmatrix} = F(\theta_t, \psi_t, s_t, a_t), \quad (90)$$

which admits unique solutions for all initial parameters, since F is uniformly Lipschitz continuous.

- Similarly, for $\beta > 1$, the proof scheme of Thm. 1 shows that discrete trajectories converge pointwise to continuous trajectories defined by the differential equation

$$\frac{d}{dt} \begin{pmatrix} \theta_t \\ \psi_t \end{pmatrix} = 0 \quad (91)$$

and thus that trajectories shrink to a single point as δt goes to 0.

We now turn to proving that when $\beta < 1$, trajectories can diverge instantly in physical time. Consider the following continuous MDP,

$$s_t = \sin(t) \quad (92)$$

whatever the actions, with reward 0 everywhere and $0 < \gamma < 1$. The resulting value function is $V(s) = 0$ (since there are no actions, V is independent of a policy), and the advantage function is 0. We consider the function approximator $V_\theta(s) = \theta s$ (which can represent the true value function). The update rule for θ is

$$\delta Q_{\delta t}^k = \gamma^{\delta t} \theta_{\delta t}^k \sin((k+1)\delta t) - \theta_{\delta t}^k \sin(k\delta t) \quad (93)$$

$$\theta_{\delta t}^{k+1} = \theta_{\delta t}^k + \alpha \delta t^\beta \frac{\gamma^{\delta t} \theta_{\delta t}^k \sin((k+1)\delta t) - \theta_{\delta t}^k \sin(k\delta t)}{\delta t} \sin(k\delta t) \quad (94)$$

Set $K_{\delta t} := \lfloor \delta t^{-\frac{\beta+3}{4}} \rfloor$, then for all $k \leq K_{\delta t}$, $o(k\delta t) = o(1)$ and

$$\theta_{\delta t}^{k+1} = \theta_{\delta t}^k (1 + \alpha \delta t^\beta (1 + o(1)) \sin(k\delta t)) \quad (95)$$

$$(96)$$

Let $\rho_{\delta t}^k := \log \theta_{\delta t}^k$. Then

$$\rho_{\delta t}^k = \rho_{\delta t}^k + \alpha k \delta t^{\beta+1} + o(k \delta t^{\beta+1}). \quad (97)$$

Finally,

$$\rho_{\delta t}^{K_{\delta t}} = \rho_{\delta t}^0 + \alpha \frac{K_{\delta t}(K_{\delta t} + 1)}{2} \delta t^\beta + o(K_{\delta t}^2 \delta t^{\beta+1}) \quad (98)$$

$$= \rho_{\delta t}^0 + \alpha \delta t^{\frac{\beta-1}{3}} + o(\delta t^{\frac{\beta-1}{3}}) \quad (99)$$

$$\xrightarrow{\delta t \rightarrow 0} +\infty. \quad (100)$$

Thus parameters diverge in an infinitesimal physical time when δt goes to 0. \square

Theorem 10. Let $F: \mathcal{S} \times \mathcal{A} \rightarrow \mathbb{R}^n$ be the dynamic, and $\pi: \mathcal{S} \times \mathcal{A} \rightarrow [0, 1]$ be the policy, such that $\pi(s, \cdot)$ is a probability distribution over \mathcal{A} . Assume that F is C^1 with bounded derivatives, and that π is C^1 and bounded. For any $\delta t > 0$, define the discretized trajectory $(s_{\delta t}^k)_k$ which amounts to sample an action from $\pi(s, \cdot)$ and maintaining each action for a time interval δt ; it is defined by induction as $s_{\delta t}^0 = s_0$, $s_{\delta t}^{k+1}$ is the value at time δt of the unique solution of

$$\frac{d\tilde{s}_t}{dt} = F(\tilde{s}_t, a_k) \quad (101)$$

with $a_k \sim \pi(s_{\delta t}^k, \cdot)$ and initial point $s_{\delta t}^k$.

Then the agent's trajectories converge when $\delta t \rightarrow 0$ to the solutions of the deterministic equation:

$$\frac{ds_t}{dt} = \mathbb{E}_{a \sim \pi(s_t, \cdot)} F(s_t, a). \quad (102)$$

Notably, if π is an epsilon greedy strategy that mixes a deterministic exploitation policy $\pi^{\text{deterministic}}$ with an action taken from a noise policy π^{noise} with probability ε at, the trajectory converge to the solutions of the equation:

$$ds_t/dt = (1-\varepsilon)F(s_t, \pi^{\text{deterministic}}(s_t)) + \varepsilon \mathbb{E}_{a \sim \pi^{\text{noise}}(a|s)} F(s_t, a) \quad (103)$$

Proof. Consider $(s_{\delta t}^k)$ the random trajectory of a near-continuous MDP with time-discretization δt^2 obtained by taking at each step k an action a_k along $a_k \sim \pi(a|s_{\delta t}^k)$ independantly. We have:

$$s_{\delta t^2}^{\lfloor 1/\delta t \rfloor} = s_{\delta t^2}^0 + \sum_{k=1}^{\lfloor 1/\delta t \rfloor} s_{\delta t^2}^k - s_{\delta t^2}^{k-1} + O(\delta t^2) \quad (104)$$

$$= s_{\delta t^2}^0 + \sum_{k=1}^{\lfloor 1/\delta t \rfloor} F(s_{\delta t^2}^{k-1}, a_{k-1}) \delta t^2 + O(\delta t^2) \quad (105)$$

We define $f(s) := \mathbb{E}_{a \sim \pi(s)} [F(s, a)] = \int_{a \in \mathcal{A}} F(s, a) \pi(s, a)$. Since π and F are bounded and C^1 , we know that f is C^1 . We have:

$$s_{\delta t^2}^{\lfloor 1/\delta t \rfloor} = s_{\delta t^2}^0 + \sum_{k=1}^{\lfloor 1/\delta t \rfloor} f(s_{\delta t^2}^{k-1}) \delta t^2 \quad (106)$$

$$+ \sum_{k=1}^{\lfloor 1/\delta t \rfloor} (F(s_{\delta t^2}^{k-1}, a_{k-1}) - f(s_{\delta t^2}^{k-1})) \delta t^2 + O(\delta t^2)$$

$$s_{\delta t^2}^{\lfloor 1/\delta t \rfloor} = s_{\delta t^2}^0 + \sum_{k=1}^{\lfloor 1/\delta t \rfloor} f(s_{\delta t^2}^{k-1}) \delta t^2 + \xi + O(\delta t^2) \quad (107)$$

with $\xi := \delta t^2 \sum_{k=1}^{\lfloor 1/\delta t \rfloor} (F(s_{\delta t^2}^{k-1}, a_{k-1}) - f(s_{\delta t^2}^{k-1}))$. By definition, we have $\mathbb{E}[\xi] = 0$. Moreover, by using the independance of actions and the boundness of F , there is $\sigma > 0$ such that:

$$\mathbb{E}[\|\xi\|^2] \leq \sigma^2 \delta t^3 \quad (108)$$

We know that f is C^1 on a compact space. Therefore, there is L_f such that f is L_f Lipschitz, and we have:

$$\left\| \left(\sum_{k=1}^{\lfloor 1/\delta t \rfloor} f(s_{\delta t^2}^{k-1}) \delta t \right) - f(s_{\delta t^2}^0) \right\| \leq \delta t L_f \sum_{k=1}^{\lfloor 1/\delta t \rfloor} \|s_{\delta t^2}^{k-1} - s_{\delta t^2}^0\| \quad (109)$$

Since F is bounded, we know that $\|s_{\delta t^2}^k - s_{\delta t^2}^{k-1}\| \leq C \delta t$. Therefore:

$$\left\| \left(\sum_{k=1}^{\lfloor 1/\delta t \rfloor} f(s_{\delta t^2}^{k-1}) \delta t \right) - f(s_{\delta t^2}^0) \right\| \leq \delta t L_f C \sum_{k=1}^{\lfloor 1/\delta t \rfloor} k \delta t \quad (110)$$

$$= O(\delta t^2) \quad (111)$$

Therefore:

$$s_{\delta t^2}^{\lfloor 1/\delta t \rfloor} = s_{\delta t^2}^0 + f(s_{\delta t^2}^0) \delta t + \xi + O(\delta t^2) \quad (112)$$

Therefore, we have $a > 0$ such that $\|s_{\delta t^2}^{\lfloor 1/\delta t \rfloor} - s_{\delta t^2}^0 - f(s_{\delta t^2}^0) \delta t\| \leq \|\xi\| + a \delta t^2$

We define $(\tilde{s}_{\delta t})$ the deterministic near-continuous process with time discretization δt defined by $\tilde{s}_{\delta t}^{k+1} := s_{\delta t}^k + f(s_{\delta t}^k)\delta t$. We have:

$$\begin{aligned} & \|s_{\delta t^2}^{(k+1)[1/\delta t]} - \tilde{s}_{\delta t}^{k+1}\| \\ & \leq \|s_{\delta t^2}^{(k+1)[1/\delta t]} - s_{\delta t^2}^{k[1/\delta t]} - f(s_{\delta t^2}^{k[1/\delta t]})\delta t\| \\ & \quad + \|s_{\delta t^2}^{k[1/\delta t]} + f(s_{\delta t^2}^{k[1/\delta t]})\delta t - \tilde{s}_{\delta t}^{k+1}\| \end{aligned} \quad (113)$$

We know that

$$\|s_{\delta t^2}^{(k+1)[1/\delta t]} - s_{\delta t^2}^{k[1/\delta t]} - f(s_{\delta t^2}^{k[1/\delta t]})\delta t\| \leq \|\xi_k\| + a\delta t^2 \quad (114)$$

Moreover:

$$\begin{aligned} & \|s_{\delta t^2}^{k[1/\delta t]} + f(s_{\delta t^2}^{k[1/\delta t]})\delta t - \tilde{s}_{\delta t}^{k+1}\| \\ & \leq \|s_{\delta t^2}^{k[1/\delta t]} - \tilde{s}_{\delta t}^k\| + \delta t \|f(s_{\delta t^2}^{k[1/\delta t]}) - f(\tilde{s}_{\delta t}^k)\| \end{aligned} \quad (115)$$

$$\leq (1 + L_f \delta t) \|s_{\delta t^2}^{k[1/\delta t]} - \tilde{s}_{\delta t}^k\| \quad (116)$$

Therefore, we have:

$$\begin{aligned} & \|s_{\delta t^2}^{(k+1)[1/\delta t]} - \tilde{s}_{\delta t}^{k+1}\| \\ & \leq \|\xi_k\| + a\delta t^2 + (1 + L_f \delta t) \|s_{\delta t^2}^{k[1/\delta t]} - \tilde{s}_{\delta t}^k\| \end{aligned} \quad (117)$$

By induction, and by taking $k = \lfloor t/\delta t \rfloor$:

$$\|s_{\delta t^2}^{k[1/\delta t]} - \tilde{s}_{\delta t}^k\| \leq \frac{a\delta t}{L_f} \exp(L_f t) + \sum_{j=0}^{\lfloor t/\delta t \rfloor} (1 + \delta t L_f)^j \|\xi_j\| \quad (118)$$

Therefore, if $\varepsilon > 0$, we have :

$$\mathbb{P}\left(\|s_{\delta t^2}^{k[1/\delta t]} - \tilde{s}_{\delta t}^k\| > \varepsilon\right) \quad (119)$$

$$\leq \mathbb{P}\left(\sum_{j=0}^{\lfloor t/\delta t \rfloor} (1 + \delta t L_f)^j \|\xi_j\| > \varepsilon - \frac{a\delta t}{L_f} \exp(L_f t)\right) \quad (120)$$

$$\leq \frac{\mathbb{E}\left[\sum_{j=0}^{\lfloor t/\delta t \rfloor} (1 + \delta t L_f)^j \|\xi_j\|\right]}{\varepsilon - \frac{a\delta t}{L_f} \exp(L_f t)} \quad (121)$$

$$\leq \frac{\mathbb{E}[\|\xi\|]}{\varepsilon - \frac{a\delta t}{L_f} \exp(L_f t)} \frac{\exp(L_f t)}{L_f \delta t} \quad (122)$$

$$(123)$$

But $\mathbb{E}[\|\xi\|] \leq \sqrt{\mathbb{E}[\|\xi\|^2]} \leq \sigma \delta t^{3/2}$. Therefore, we have:

$$\mathbb{P}\left(\|s_{\delta t^2}^{\lfloor t/\delta t \rfloor [1/\delta t]} - \tilde{s}_{\delta t}^k\| > \varepsilon\right) = O(\sqrt{\delta t}) \quad (124)$$

Therefore, the process $t \mapsto s_{\delta t^2}^{\lfloor t/\delta t \rfloor [1/\delta t]}$ converges in probability to \tilde{s} . Furthermore, by a similar argument than in

Lemma 1, we know that the discretized process \tilde{s} converge to the continuous process defined by $\frac{ds}{dt} = f(s_t)$. We can conclude our result. \square

B. Implementation details

All the details specifying our implementation are given in this section. We first give precise pseudo code descriptions for both *Continuous Deep Advantage Updating* (Alg. 2), as well as the variants of DDPG (Alg. 3) and DQN (Alg. 4) used.

Algorithm 2 Continuous DAU

Inputs:

θ, ψ and ϕ , parameters of V_θ, \bar{A}_ψ and π_ϕ .

π^{explore} and $\nu_{\delta t}$ defining an exploration policy.

$\text{opt}_V, \text{opt}_A, \text{opt}_\pi, \alpha^V \delta t, \alpha^A \delta t$ and $\alpha^\pi \delta t$, optimizers and learning rates.

\mathcal{D} , buffer of transitions (s, a, r, d, s') , with d the episode termination signal.

δt and γ , time discretization and discount factor.

nb_epochs number of epochs.

nb_steps, number of steps per epoch.

Observe initial state s^0

$t \leftarrow 0$

for $e = 0, \text{nb_epochs}$ **do**

for $j = 1, \text{nb_steps}$ **do**

$a^k \leftarrow \pi^{\text{explore}}(s^k, \nu_{\delta t}^k)$.

 Perform a^k and observe $(r^{k+1}, d^{k+1}, s^{k+1})$.

 Store $(s^k, a^k, r^{k+1}, d^{k+1}, s^{k+1})$ in \mathcal{D} .

$k \leftarrow k + 1$

end for

for $k = 0, \text{nb_learn}$ **do**

 Sample a batch of N random transitions from \mathcal{D}

$Q^i \leftarrow V_\theta(s^i) + \delta t (\bar{A}_\psi(s^i, a^i) - \bar{A}_\psi(s^i, \pi_\phi(s^i)))$

$\tilde{Q}^i \leftarrow r^i \delta t + (1 - d^i) \gamma^{\delta t} V_\theta(s^i)$

$\Delta \theta \leftarrow \frac{1}{N} \sum_{i=1}^N \frac{(Q^i - \tilde{Q}^i) \partial_\theta V_\theta(s^i)}{\delta t}$

$\Delta \psi \leftarrow \frac{1}{N} \sum_{i=1}^N \frac{(Q^i - \tilde{Q}^i) \partial_\psi (\bar{A}_\psi(s^i, a^i) - \bar{A}_\psi(s^i, \pi_\phi(s^i)))}{\delta t}$

$\Delta \phi \leftarrow \frac{1}{N} \sum_{i=1}^N \partial_a \bar{A}_\psi(s^i, \pi_\phi(s^i)) \partial_\phi \pi_\phi(s^i)$

 Update θ with $\text{opt}_V, \Delta \theta$ and learning rate $\alpha^V \delta t$.

 Update ψ with $\text{opt}_A, \Delta \psi$ and learning rate $\alpha^A \delta t$.

 Update ϕ with $\text{opt}_\pi, \Delta \phi$ and learning rate $\alpha^\pi \delta t$.

end for

end for

For DDPG and DQN, two different settings were experimented with:

Algorithm 3 DDPG

Inputs:

ψ and ϕ , parameters of Q_ψ and π_ϕ .
 ψ' and ϕ' , parameters of target networks $Q_{\psi'}$ and $\pi_{\phi'}$.
 π^{explore} and ν defining an exploration policy.
 opt_Q , opt_π , α^Q and α^π , optimizers and learning rates.
 \mathcal{D} , buffer of transitions (s, a, r, d, s') , with d the episode termination signal.
 γ discount factor.
 τ target network update factor.
nb_epochs number of epochs.
nb_steps, number of steps per epoch.

Observe initial state s^0

$t \leftarrow 0$

for $e = 0, \text{nb_epochs}$ **do**

for $j = 1, \text{nb_steps}$ **do**

$a^k \leftarrow \pi^{\text{explore}}(s^k, \nu^k)$.

 Perform a^k and observe $(r^{k+1}, d^{k+1}, s^{k+1})$.

 Store $(s^k, a^k, r^{k+1}, d^{k+1}, s^{k+1})$ in \mathcal{D} .

$k \leftarrow k + 1$

end for

for $k = 0, \text{nb_learn}$ **do**

 Sample a batch of N random transitions from \mathcal{D}

$\tilde{Q}^i \leftarrow r^i + (1 - d^i)\gamma Q_{\psi'}(s^i, \pi_{\phi'}(s^i))$

$\Delta\psi \leftarrow \frac{1}{N} \sum_{i=1}^N \left(Q^i - \tilde{Q}^i \right) \partial_\psi Q(s^i, a^i)$

$\Delta\phi \leftarrow \frac{1}{N} \sum_{i=1}^N \partial_a Q_\psi(s^i, \pi_\phi(s^i)) \partial_\phi \pi_\phi(s^i)$

 Update ψ with opt_Q , $\Delta\psi$ and learning rate α^Q .

 Update ϕ with opt_π , $\Delta\phi$ and learning rate α^π .

$\psi' \leftarrow \tau\psi' + (1 - \tau)\psi$

$\phi' \leftarrow \tau\phi' + (1 - \tau)\phi$

end for

end for

Algorithm 4 DQN

Inputs:

ψ parameter of Q_ψ .
 ψ' , parameters of target networks $Q_{\psi'}$.
 π^{explore} and ν defining an exploration policy.
 opt_Q , α^Q optimizer and learning rate.
 \mathcal{D} , buffer of transitions (s, a, r, d, s') , with d the episode termination signal.
 γ discount factor.
 τ target network update factor.
nb_epochs number of epochs.
nb_steps, number of steps per epoch.

Observe initial state s^0

$t \leftarrow 0$

for $e = 0, \text{nb_epochs}$ **do**

for $j = 1, \text{nb_steps}$ **do**

$a^k \leftarrow \pi^{\text{explore}}(s^k, \nu^k)$.

 Perform a^k and observe $(r^{k+1}, d^{k+1}, s^{k+1})$.

 Store $(s^k, a^k, r^{k+1}, d^{k+1}, s^{k+1})$ in \mathcal{D} .

$k \leftarrow k + 1$

end for

for $k = 0, \text{nb_learn}$ **do**

 Sample a batch of N random transitions from \mathcal{D}

$\tilde{Q}^i \leftarrow r^i + (1 - d^i)\gamma \max_{a'} Q_{\psi'}(s^i, a')$

$\Delta\psi \leftarrow \frac{1}{N} \sum_{i=1}^N \left(Q^i - \tilde{Q}^i \right) \partial_\psi Q(s^i, a^i)$

 Update ψ with opt_Q , $\Delta\psi$ and learning rate α^Q .

$\psi' \leftarrow \tau\psi' + (1 - \tau)\psi$

end for

end for

- One with time discretization scalings, to keep the comparison fair. In this setting, the discount factor is still scaled as $\gamma^{\delta t}$, rewards are scaled as $r\delta t$, and learning rates are scaled to obtain parameter updates of order δt . As RMSprop is used for all experiments, this amounts to using a learning rate scaling as $\alpha^Q = \tilde{\alpha}^Q \delta t$, $\alpha^\pi = \tilde{\alpha}^\pi \delta t$.
- One without discretization scalings. In that case, only the discount factor is scaled as $\gamma^{\delta t}$, to prevent unfair shortsightedness. All other parameters are set with a reference $\delta t_0 = 1e - 2$. For instance, for all δt 's, the reward perceived is $r * \delta t_0$, and similarly for learning rates, $\alpha^Q = \tilde{\alpha}^Q \delta t_0$, $\alpha^\pi = \tilde{\alpha}^\pi \delta t_0$. These scalings don't depend on the discretization, but perform decently at least for the highest discretization.

B.1. Global hyperparameters

The following hyperparameters are maintained constant throughout all our experiments,

- All networks used are of the form

```
Sequential (
  Linear (nb_inputs, 256),
  LayerNorm (256),
  ReLU (),
  Linear (256, 256),
  LayerNorm (256),
  ReLU (),
  Linear (256, nb_outputs)
) .
```

Policy networks have an additional tanh layer to constraint action range. On certain environments, network inputs are normalized by applying a mean-std normalization, with mean and standard deviations computed on each individual input features, on all previously encountered samples.

- \mathcal{D} is a cyclic buffer of size 1000000.
- **nb_steps** is set to 10, and 256 environments are run in parallel to accelerate the training procedure, totalling 2560 environment interactions between learning steps.
- **nb_learn** is set to 50.
- The physical γ is set to 0.8. It is always scaled as $\gamma^{\delta t}$ (even for unscaled DQN and DDPG).
- N , the batch size is set to 256.
- RMSprop is used as an optimizer without momentum, and with $\alpha = 1 - \delta t$ (or $1 - \delta t_0$ for unscaled DDPG and DQN).

- Exploration is always performed as described in the main text. The OU process used as parameters $\kappa = 7.5$, $\sigma = 1.5$.
- Unless otherwise stated, $\alpha_1 := \tilde{\alpha}^Q = \alpha^V = \alpha^A = 0.1$, $\alpha_2 := \tilde{\alpha}^\pi = \alpha^\pi = 0.03$.
- $\tau = 0.9$

B.2. Environment dependent hyperparameters

We hereby list the hyperparameters used for each environment. Continuous actions environments are marked with a (C), discrete actions environments with a (D).

- **Ant (C)**: State normalization is used. Discretization range: [0.05, 0.02, 0.01, 0.005, 0.002].
- **Cheetah (C)**: State normalization is used. Discretization range: [0.05, 0.02, 0.01, 0.005, 0.002]
- **Bipedal Walker (C)**⁵: State normalization is used, $\alpha_2 = 0.02$. Discretization range: [0.01, 0.005, 0.002, 0.001].
- **Cartpole (D)**: $\alpha_2 = 0.02$, $\tau = 0$. Discretization range: [0.01, 0.005, 0.002, 0.001, 0.0005].
- **Pendulum (C)**: $\alpha_2 = 0.02$, $\tau = 0$. Discretization range: [0.01, 0.005, 0.002, 0.001, 0.0005].

C. Additional results

Additional results mentioned in the text are presented in this section.

⁵ The reward for Bipedal Walker is modified not to scale with δt . This does not introduce any change for the default setup.

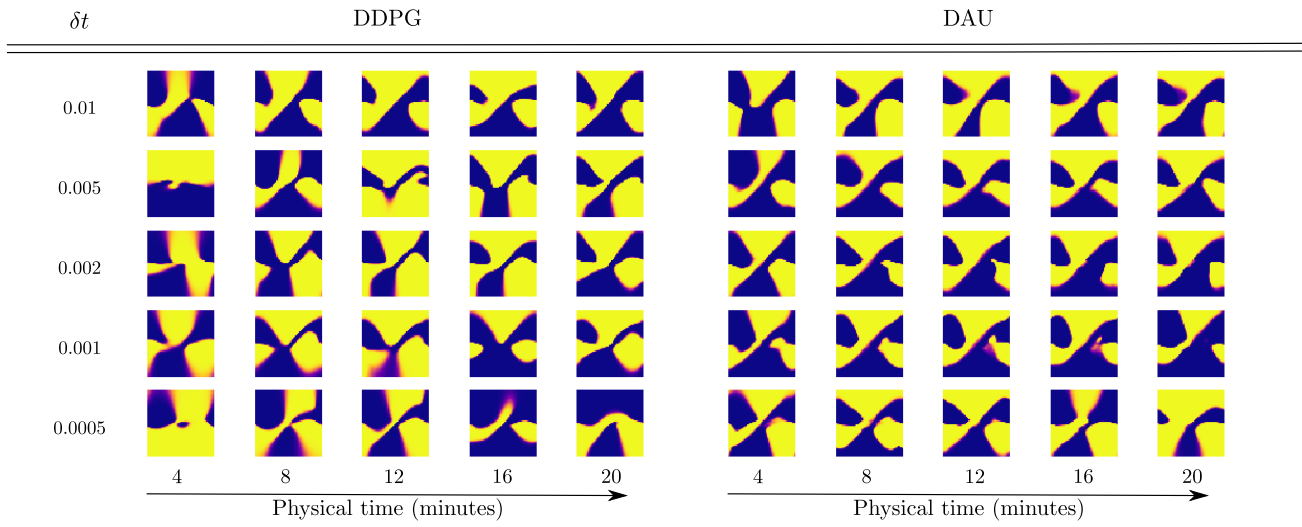


Figure 3. Policies obtained by DDPG (unscaled version) and AU at different instants in physical time of training on the pendulum swing-up environment. Each image represents the policy learnt by the policy network, with x -axis representing angle, and y -axis angular velocity. The lighter the pixel, the closer to 1 the action, the darker, the closer to -1 .

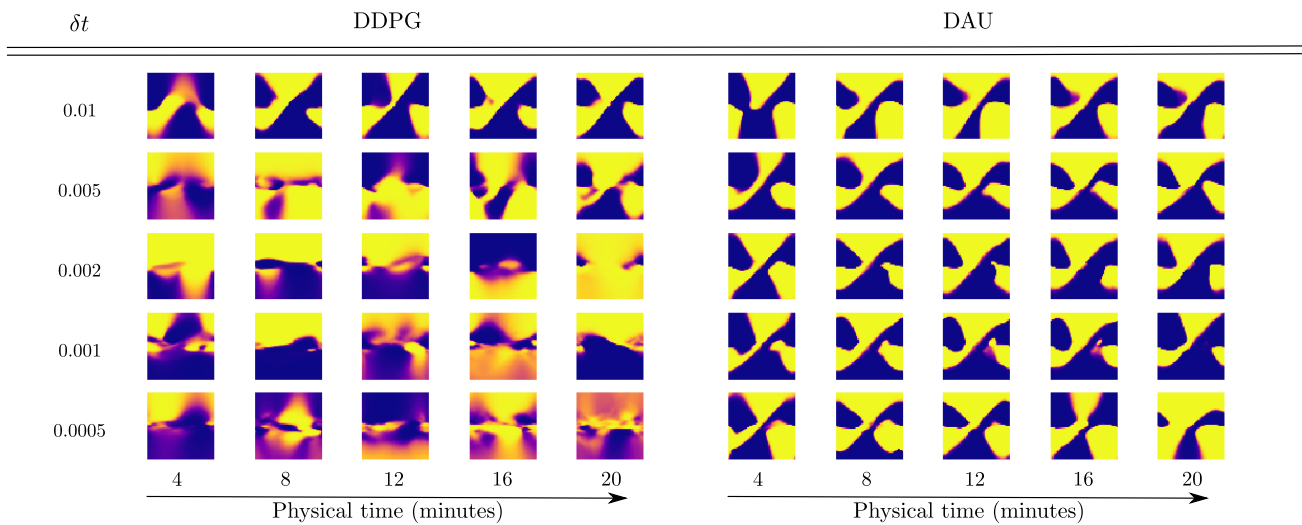


Figure 4. Policies obtained by DDPG (scaled version) and AU at different instants in physical time of training on the pendulum swing-up environment. Each image represents the policy learnt by the policy network, with x -axis representing angle, and y -axis angular velocity. The lighter the pixel, the closer to 1 the action, the darker, the closer to -1 .

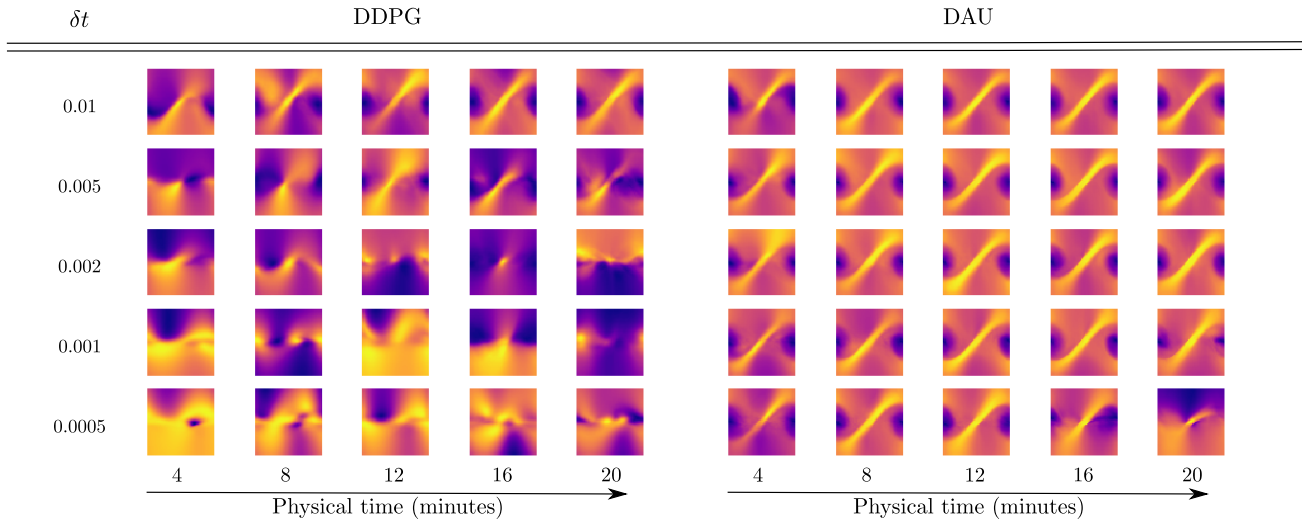


Figure 5. Value functions obtained by DDPG (scaled version) and AU at different instants in physical time of training on the pendulum swing-up environment. Each image represents the value function learnt, with x -axis representing angle, and y -axis angular velocity. The lighter the pixel, the higher the value.

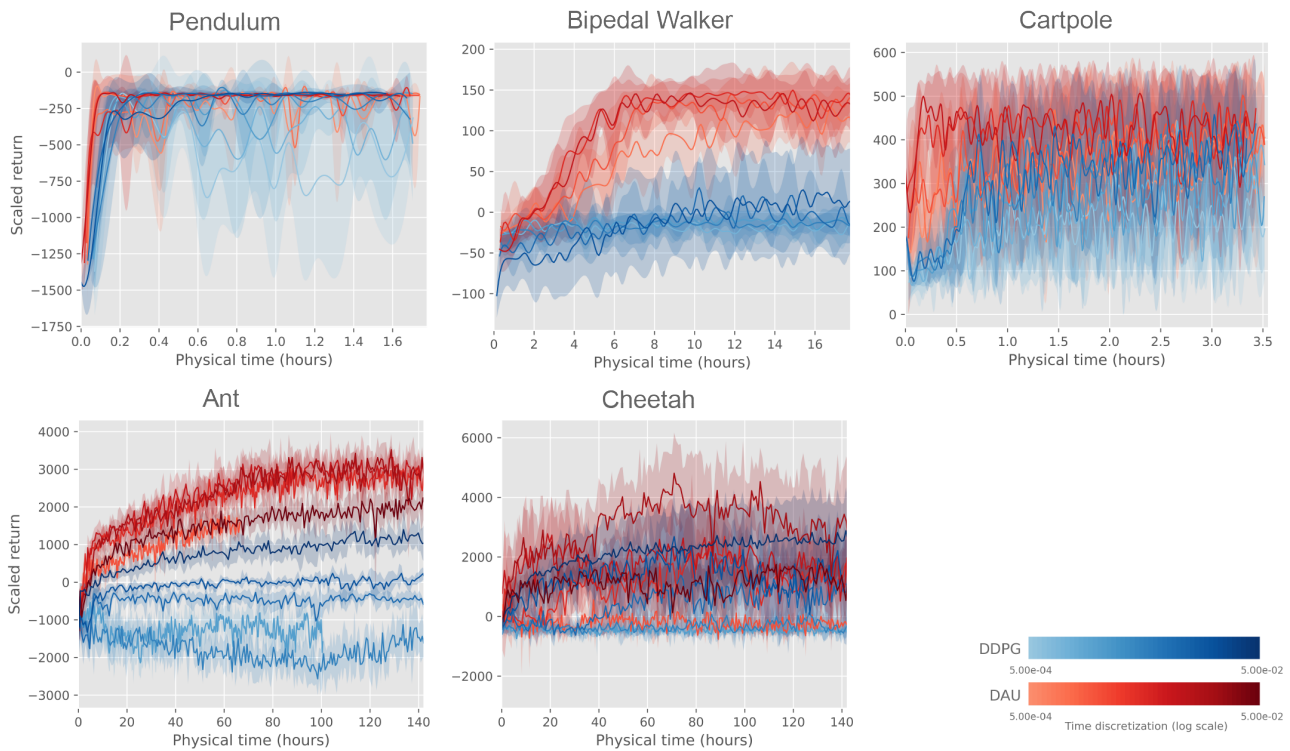


Figure 6. Learning curves for DAU and DDPG (scaled) on classic control benchmarks for various time discretization δt : Scaled return as a function of the physical time spent in the environment.